

1 **Factor V is an immune inhibitor that is expressed at increased levels in leukocytes of patients with**  
2 **severe Covid-19**

3

4 Jun Wang<sup>1</sup>, Prasanti Kotagiri<sup>1,2</sup>, Paul A Lyons<sup>1,2</sup>, Federica Mescia<sup>1,2</sup>, Laura Bergamaschi<sup>1,2</sup>, Lorinda  
5 Turner<sup>1,2</sup>, Rafia S Al-Lamki<sup>1,3</sup>, Michael D Morgan<sup>5,12</sup>, Fernando J Calero-Nieto<sup>6</sup>, Karsten Bach<sup>5,7</sup>, Nicole  
6 Mende<sup>6</sup>, Nicola K Wilson<sup>6</sup>, Emily R Watts<sup>8</sup>, Cambridge Institute of Therapeutic Immunology and  
7 Infectious Disease-National Institute of Health Research (CITIID-NIHR) COVID BioResource  
8 Collaboration, Patrick F Chinnery<sup>9,10,11</sup>, Nathalie Kingston<sup>9,12</sup>, Sofia Papadia<sup>9,13</sup>, Kathleen Stirrups  
9 PhD<sup>9,12</sup>, Neil Walker<sup>9,12</sup>, Ravindra K Gupta<sup>1,2</sup>, Mark Toshner<sup>1,14</sup>, Michael P Weekes<sup>1</sup>, James A Nathan<sup>1,2</sup>,  
10 Sarah R Walmsley<sup>8</sup>, Willem H Ouwehand<sup>6,9,15</sup>, Mary Kasanicki<sup>3</sup>, Berthold Göttgens<sup>6</sup>, John C  
11 Marioni<sup>4,5,16</sup>, Kenneth GC Smith<sup>1,2</sup>, Jordan S Pober<sup>1,17</sup>, John R Bradley<sup>1,3,9</sup>.

12

13

- 14 1. Department of Medicine, University of Cambridge, Cambridge Biomedical Campus, CB2
- 15 0QQ, UK
- 16 2. Cambridge Institute of Therapeutic Immunology and Infectious Disease, Jeffrey Cheah
- 17 Biomedical Centre, University of Cambridge, Cambridge CB2 0AW, UK
- 18 3. Cambridge University Hospitals NHS Foundation Trust, Addenbrooke's Hospital, Cambridge
- 19 CB2 0QQ, UK
- 20 4. Wellcome Sanger Institute, Wellcome Genome Campus, Hinxton, Cambridge, UK
- 21 5. Cancer Research UK – Cambridge Institute, Robinson Way, Cambridge, CB2 0RE, UK
- 22 6. Department of Haematology, Wellcome & MRC Cambridge Stem Cell Institute, University of
- 23 Cambridge, Cambridge, Cambridgeshire, England CB2 0AW, UK
- 24 7. Department of Pharmacology, University of Cambridge, Cambridge, CB2 1PD, UK
- 25 8. Centre for Inflammation Research, Queen's Medical Research Institute, University of
- 26 Edinburgh, Edinburgh, EH16 4TJ, UK
- 27 9. NIHR BioResource, Cambridge University Hospitals NHS Foundation, Cambridge Biomedical
- 28 Campus, Cambridge CB2 0QQ, UK
- 29 10. Department of Clinical Neurosciences, School of Clinical Medicine, University of Cambridge,
- 30 Cambridge Biomedical Campus, Cambridge, CB2 0QQ, UK.
- 31 11. Medical Research Council Mitochondrial Biology Unit, University of Cambridge, Cambridge
- 32 Biomedical Campus, Cambridge, CB2 0XY, UK
- 33 12. Department of Haematology, School of Clinical Medicine, University of Cambridge,
- 34 Cambridge Biomedical Campus, Cambridge, CB2 0QQ, UK.
- 35 13. Department of Public Health and Primary Care, School of Clinical Medicine, University of
- 36 Cambridge, Cambridge Biomedical Campus, Cambridge, CB2 0QQ, UK.
- 37 14. Royal Papworth Hospital NHS Foundation Trust, Papworth Road, Cambridge CB2 0AY, UK
- 38 15. NHS Blood and Transplant, Cambridge Biomedical Campus, Cambridge, CB2 0PT, UK
- 39 16. EMBL-EBI, Wellcome Genome Campus, Hinxton, CB10 1SD, UK
- 40 17. Department of Immunobiology, Yale University School of Medicine, New Haven,
- 41 Connecticut, CT 06519, USA.

42

43 Corresponding author:

44 Professor John R Bradley

45 Box 118 Addenbrooke's Hospital Cambridge CB2 0QQ

46 [jrb1000@cam.ac.uk](mailto:jrb1000@cam.ac.uk)

47 +44 7710905570

48

49

NOTE: This preprint reports new research that has not been certified by peer review and should not be used to guide clinical practice.

50

51 **Abstract**

52

53 Severe Covid-19 is associated with elevated plasma Factor V (FV) and increased risk of  
54 thromboembolism. We report that neutrophils, T regulatory cells (Tregs), and monocytes from  
55 patients with severe Covid-19 express FV, and expression correlates with T cell lymphopenia. *In vitro*  
56 full length FV, but not FV activated by thrombin cleavage, suppresses T cell proliferation. Increased  
57 and prolonged FV expression by cells of the innate and adaptive immune systems may contribute to  
58 lymphopenia in severe Covid-19. Activation by thrombin destroys the immunosuppressive properties  
59 of FV. Anticoagulation in Covid-19 patients may have the unintended consequence of suppressing  
60 the adaptive immune system.

61 **Introduction**

62

63 Dysregulation of both the immune<sup>1</sup> and coagulation system<sup>2</sup> occurs in Covid-19 infection.

64 Immunological responses include T cell lymphopenia, which we have found can persist for months

65 after the initial illness. Coagulopathy is an important cause of morbidity and mortality in patients

66 with Covid-19, and a marked increase in circulating FV activity has been reported in patients with

67 severe Covid-19, associated with increased risk of thromboembolism<sup>3</sup>.

68

69 Production of FV by T cells<sup>4</sup> and monocytes<sup>5</sup> has been previously reported. We report that circulating

70 leukocytes are a source of FV in patients with Covid-19, and propose that neutrophil, monocyte and

71 Treg derived Factor V may be an important determinant of the dysregulated immune response to

72 SARS-CoV-2.

73

## 74 **Results**

75

### 76 FV is produced by circulating blood cells and increased in hospitalised patients with Covid-19

77 Analysis of the transcriptome of peripheral blood cells from healthy controls and patients with  
78 Covid-19 express FV, and expression is increased in patients with more severe disease for at least 60  
79 days after onset of symptoms (Figure 1A). Analysis of the Blueprint ([https://www.blueprint-  
80 epigenome.eu/](https://www.blueprint-epigenome.eu/)) database of haematopoietic genome-scale datasets shows the highest level of FV  
81 expression in neutrophils, eosinophils, Tregs and monocytes (Supplementary Figure 1). To  
82 investigate whether Tregs and monocytes express FV in patients with Covid-19 we performed  
83 scRNAseq on peripheral blood mononuclear cells (PBMCs) derived from healthy controls and  
84 patients with Covid19. Tregs (CD4+, FoxP3+) had the highest expression of FV, with expression also  
85 detected in monocytes and lower levels in other CD4 cell subsets (Figure 1B). However, expression in  
86 PBMCs did not appear to correlate with disease severity. Expression of FV in Tregs from healthy  
87 controls was confirmed by RT-PCR and immunoblotting (Supplementary Figure 2).

88

### 89 Neutrophils are a source of increased FV expression in patients with severe Covid-19

90 Weighted gene co-expression network analysis was performed to create distinct modules comprising  
91 of non-overlapping co-expressed genes. The module containing FV also contained genes strongly  
92 expressed in neutrophils (Figure 2A, Supplementary Figure 3). In addition, FV was a “hub gene”  
93 meaning its expression closely mirrored that of the module eigengene, which is a single expression  
94 profile summarising all genes within the module. This FV module eigengene expression correlated  
95 with severity of Covid-19 (Figure 2B). FV module expression is similar to healthy controls in  
96 asymptomatic or mildly symptomatic individuals in the community. In hospitalised patients with mild  
97 disease FV module expression is elevated at presentation, but declines as patients recover. In  
98 patients with severe disease FV module expression is elevated at presentation and increased levels  
99 persists for several weeks. Analysis of peripheral blood cells for expression of other coagulation

100 factors showed expression of Factor XIIIa and low levels of Factor XII but not other coagulation  
101 factors (data not shown).

102 To determine whether increased peripheral blood cell FV mRNA levels correlate with FV protein  
103 expression we assayed plasma FV levels and performed liquid chromatography – mass spectrometry  
104 on neutrophil lysates from healthy controls and patients with severe Covid-19. There was a modest  
105 but statistically significant correlation between FV gene expression and FV protein expression (Figure  
106 3A;  $p = 0.023$ ,  $R = 0.17$ ). Proteomic analysis showed significantly higher levels of FV in neutrophil  
107 lysates from patients with severe Covid-19 compared to healthy controls (Figure 3B).

108

#### 109 FV expression correlates with parameters of disease severity and lymphopenia

110 FV module gene expression correlates with suppression of T cell counts during the first 24 days after  
111 symptom onset (Figure 3C.iv), and T and B cell counts after 24 days from the onset of symptoms  
112 (Figure 3C.vi). In contrast, there was very little correlation between plasma factor V levels and T and  
113 B cell counts during the first 24 days after symptom onset (Figure 3C.iii) or after 24 days from the  
114 onset of symptoms (Figure 3C.v). FV module gene expression correlated with predictors of disease  
115 severity (age, male gender, CRP) and increased plasma levels of IL6, IL10 and TNF, but not clinical  
116 parameters including laboratory measurements of haemostasis (Figure 3C.ii), whereas FV plasma  
117 levels correlate with laboratory measures of haemostasis (Figure 3C.i).

118

#### 119 FV suppresses T cell proliferation

120 The high level of expression of FV in Tregs led us to determine if FV suppresses *in vitro* proliferation  
121 of T cells. To examine this, CFSE-labelled conventional CD4<sup>+</sup> T cells (Tcons) from healthy donors were  
122 stimulated *in vitro* and proliferation was assessed by flow cytometry analysis of dye dilution. FV but  
123 not FV activated by thrombin (FVa) suppressed proliferation of Tcons in a concentration dependent  
124 manner (Figure 4). To confirm that the suppressive effect was mediated by full length uncleaved FV  
125 we generated recombinant proteins from three FV constructs: (1) FV(738-1573)-6His (the B domain

126 of FV); (2) FV-6His (full length Factor V); (3) Factor V R709A, R1018A, R1545A-6His (full length FV  
127 with Arginine thrombin cleavage sites mutated). Full length recombinant FV, but not a recombinant  
128 B domain, inhibited Tcon proliferation, and this effect was prevented by thrombin, and enhanced by  
129 the thrombin inhibitor hirudin (Figure 5A). Thrombin did not increase proliferation in the absence of  
130 FV. A cleavage resistant recombinant FV was a potent inhibitor of Tcon proliferation. Recombinant  
131 full length FV and a cleavage resistant recombinant FV also suppress CD8+ T cell proliferation, but  
132 not B cell proliferation (Figure 5B).

133

134 **Discussion**

135

136 Covid-19 is associated with an increased risk of venous thromboembolism (VTE), particularly in  
137 patients with severe illness. Abnormalities of the coagulation system are likely to contribute to the  
138 increased risk, and the most consistent laboratory finding is an increased D-dimer level, with some  
139 reports of prolongation of the prothrombin time and thrombin time, and shortened activated partial  
140 thromboplastin time<sup>6,7</sup>. FV levels are increased in Covid-19<sup>8</sup>, and marked increases in FV activity have  
141 been associated with VTE in some patients with severe Covid-19<sup>3</sup>.

142

143 Our data show that circulating neutrophils, monocytes and Tregs are a source of FV in patients with  
144 severe Covid-19, and also identify Tregs as a source of FV in healthy blood donors. Furthermore FV  
145 decreases T cell proliferation *in vitro*. This suppression of T cell responses is lost if FV is activated by  
146 thrombin, and potentiated by a recombinant FV in which thrombin cleavage sites are mutated to  
147 prevent activation. In patients with Covid-19 increased circulating blood cell FV expression is  
148 associated with suppression of T cell counts, and both increased FV expression and suppressed T cell  
149 subsets can persist for several months after infection with SARS-CoV-2.

150

151 There was a modest but statistically significant correlation between FV gene expression in circulating  
152 blood cells and plasma FV levels, but the key role of leukocyte derived FV in regulating the immune  
153 response to SARS-CoV-2 is likely to occur following migration of leukocytes into the tissues, including  
154 secondary lymphoid organs from which circulating FV is normally excluded. Broncho-alveolar lavage  
155 fluid from patients with severe Covid-19 has shown a predominance of neutrophils,  
156 monocytes/macrophages, and eosinophils with few lymphocytes, and in particular CD4 and CD8 T  
157 cell lymphopenia, but an increase in the proportion of Tregs<sup>9</sup>. Furthermore lymphocytes were either  
158 absent or sparse in areas of SARS-CoV-2 pneumonia infiltrated by macrophages or neutrophils, or  
159 containing neutrophil extracellular traps (NETs) composed of neutrophil DNA, histones and granule-

160 derived enzymes<sup>10,11</sup>. Thus leukocyte derived FV may suppress local T cell proliferation at sites of  
161 infection. In support of this plasma FV levels correlated with biomarkers of haemostasis, whereas T  
162 cell counts correlated with FV module gene expression in circulating leukocytes. The liver may be the  
163 predominant source of circulating FV, and it is noteworthy that the liver displays adaptive immune  
164 tolerance<sup>12</sup>.

165  
166 Guidelines recommend unfractionated heparin (UFH) or low molecular weight heparin (LMWH) as  
167 prophylaxis against VTE in Covid-19<sup>13</sup>. Heparin binds to and activates anti-thrombin<sup>14</sup>. LMWHs retain  
168 some anti-thrombin activity, but most of their activity is thought to result from inhibition of Factor  
169 Xa<sup>15</sup>. Alternatives for VTE prophylaxis include warfarin and direct oral anticoagulants (DOACs).  
170 Warfarin depletes the reduced form of vitamin K that acts as a cofactor for gamma carboxylation of  
171 prothrombin, VII, IX and X, rendering them inactive<sup>16</sup>. DOACs inhibit factor Xa or thrombin. The  
172 effect of anticoagulants on circulating factor V levels is unknown, but by inhibiting thrombin heparin  
173 reduces factor V activation, and could potentiate the T cell suppressive effect of FV. In support of  
174 this there is evidence that heparin can directly suppress immune, and in particular T cell,  
175 responses<sup>17</sup>. Prophylaxis against VTE is an essential for the management of hospitalised patients  
176 with Covid-19. Increased FV expression by cells of the innate and adaptive immune systems may  
177 explain the lymphopenia seen in patients with severe Covid19. Heparin may potentiate suppression  
178 of the adaptive immune response by reducing FV activation.

179

180

181

182

183



184 **Methods**

185

186 **Materials.** Rabbit anti-human FoxP3 (Cell signalling technology, Hitchin, UK). Mouse anti-human FV  
187 (Cambridge Biosciences, Cambridge, UK). B cell proliferation kit (R&D system, Abingdon, UK). BD  
188 CellFix (BD Biosciences, Oxford, UK). Proteinase inhibitor cocktail (Roche Diagnostics Ltd, West  
189 Sussex, UK). Native human FV, FVa, Thrombin, Dynabeads Human T cell activator, PCR kits,  
190 CYBRgreen kit and CFSE kits (Thermofisher Scientific, Loughborough, UK). CD4+CD25 + CD127- T reg,  
191 CD8 T cell and B cell isolation kit (Miltenyi Biotec, Surrey, UK). Assay of FV plasma levels was  
192 performed using a human Factor V ELISA Kit (ab137976, Abcam, Cambridge, UK). Unless otherwise  
193 indicated, all reagents were from Sigma-Aldrich Company Ltd (Dorset, UK).

194

195 **Healthy volunteers and patients**

196 Healthy donor blood samples were obtained from the NIHR Cambridge BioResource and  
197 leukapheresis samples from the National Health Service Blood and Transfusion services (NHSBT,  
198 Cambridge) with written informed consent of donors and approval of the National Research Ethics  
199 Committee and Health Research Authority. Healthcare workers and patients with Covid-19  
200 confirmed by Nucleic acid amplification testing<sup>18</sup> of nasopharyngeal swabs for SARS-CoV-2 were  
201 consented to the NIHR Covid-19 cohort of the NIHR BioResource  
202 (<https://cambridgebc.nihr.ac.uk/bioresourcecovid19/>) with approval of the National Research  
203 Ethics Committee and Health Research Authority. These included patients presenting to Cambridge  
204 University Hospitals and Royal Papworth Hospital, together with asymptomatic or symptomatic  
205 healthcare workers (HCWs) undergoing routine screening. Samples were also collected from  
206 seronegative concurrent controls recruited. Hospitalised patients underwent a venous  
207 thromboembolism risk assessment and received prophylactic dalteparin if there was low bleeding

208 risk. From 1 May 2020 patients were discharged with 2 weeks of prophylactic dalteparin following a  
209 risk assessment.

210 For neutrophil proteomic studies peripheral venous blood was taken from healthy volunteers (age  
211 25 – 60, one female) with written informed and approval of the University of Edinburgh Centre for  
212 Inflammation Research Blood Resource Management Committee. The collection of peripheral  
213 venous blood from patients (age 41 – 56, one female) with Covid-19 was approved by Scotland A  
214 Research Ethics Committee. Patients receiving ventilation in intensive care at the Royal Infirmary of  
215 Edinburgh were recruited between April and August 2020, with informed consent obtained by proxy.

216

### 217 **Peripheral blood cell isolation**

218 PBMCs were isolated from blood by polysucrose density gradient centrifugation (Ficoll-Paque, GE  
219 Healthcare Life Sciences, UK). Cells were grown in RPMI media supplemented with 10% human AB  
220 serum.

221 Neutrophils were isolated from blood by dextran sedimentation and discontinuous Percoll gradients.

222 Analysis of neutrophil lysates was performed using liquid chromatography mass spectrometry (LC-  
223 MS)-based proteomics

224

225 **T cell *in vitro* expansion assay.** Tcons were isolated with the above-mentioned kit. Cells were stained  
226 with CFSE following the manufacturer's instruction.  $5 \times 10^4$  labelled T cons were mixed with  
227 Dynabeads Human T cell activator CD3/CD28 at cell-to-beads ratio of 2 to 1. Cells were collected and  
228 analysed using a BD Fortessa flow cytometer after 4 or 5 days. Suppression index was calculated as  
229 the ratio between decreased percentage of proliferation and the total percentage of proliferation of  
230 the cells.

231 Flow cytometry data were analysed using FlowJo (Tree Star, USA). Graphs and statistics were  
232 generated using GraphPad Prism software. Results were presented as mean  $\pm$  s.e.m.as indicated.

233 Differences between two groups were compared using two-tailed student's t-test.

## 234 **Whole blood bulk mRNA-Seq**

### 235 Library preparation and RNA-Seq processing

236 RNA was quantified using RNA HS assay on the Qubit, and libraries prepared using the SMARTer®  
237 Stranded Total RNA-Seq it v2 - Pico Input Mammalian kit (Takara) with 10ng of RNA as starting input.  
238 Library quality and quantity were validated by capillary electrophoresis on an Agilent 4200  
239 TapeStation. Libraries were pooled at equimolar concentrations, and paired-end sequenced (75bp)  
240 across 4 lanes of a Hiseq4000 instrument (Illumina) to achieve 10 million reads per samples.

### 241 Reads mapping and quantification

242 The quality of raw reads was assessed using FastQC  
243 (<http://www.bioinformatics.babraham.ac.uk/projects/fastqc/>). SMARTer adaptors were trimmed,  
244 along with sequencing calls with a Phred score below 24 using Trim\_galore v.0.6.4  
245 ([http://www.bioinformatics.babraham.ac.uk/projects/trim\\_galore/](http://www.bioinformatics.babraham.ac.uk/projects/trim_galore/).) Residual rRNA reads were  
246 depleted in silico using BBSplit (<https://github.com/BioInfoTools/BBMap/blob/master/sh/bbsplit.sh>).  
247 Alignment was performed using HISAT2 v.2.1.0<sup>19</sup> against the GRCh38 genome build achieving a more  
248 than 95% alignment rate. A count matrix was generated in R using featureCounts (Rsubreads -  
249 packages) and converted into a DGEList (EdgeR package), for downstream analysis.

### 250 Downstream Analysis

251 Downstream analysis was performed in R. Counts were filtered using filterByExpr (EdgeR package)  
252 with a gene count threshold of 10CPM and the minimum number of samples set as the size of the  
253 smallest disease group. Library counts were normalised using calcNormFactors (EdgeR package)  
254 using the method 'weighted trimmed mean of M-values'. The function 'voom' (limma package) was  
255 applied to the data to estimate the mean-variance relationship, allowing adjustment for  
256 heteroscedasticity.

### 257 Weighted gene co-expression network analysis

258 The weighted gene co-expression network analysis (WGCNA) package in R overcomes the problem  
259 of multiple testing by grouping co-correlated genes into modules and relating them to clinic traits.

260 Modules are not comprised of a priori defined gene sets but rather are generated from unsupervised  
261 clustering. The eigengene of the module is then correlated with the sample traits and significance  
262 determined. A signed adjacency matrix was generated, and a soft thresholding power chosen to  
263 impose approximate scale-free topology. Modules identified from the topological overlap matrix had  
264 a specified minimum module size of 30. Significance of correlation between a clinical trait and a  
265 modular eigengene was assessed using linear regression with Bonferroni adjustment to correct for  
266 multiple testing. Modules were annotated using Enrichr and Genemania. Genes with high  
267 connectivity termed “hub genes” were identified based on a module membership of 0.8 or above  
268 and were selected to have a correlation with the trait of interest  $\geq 0.8$ .

#### 269 Correlation

270 The relationships between multiple features were quantified using Pearson’s correlation (Hmisc  
271 package) and visualized with corrplot.

#### 272 Mixed Effects model

273 Longitudinal mixed modelling of factor V module eigenvalue changes over time ( $y_{ij}$ ) was conducted  
274 using the nlme package in R, including time ( $t_{ij}$ ) with a quadratic trend and disease severity ( $X_j$ ) as  
275 fixed effects, and sampled individuals as random effects ( $u_j$ ).

276

#### 277 **scRNAseq of PBMCs**

##### 278 Sample processing and antibody staining

279 Pools of purified PBMCs were generated by combining 0.5 million live cells from four individuals and  
280 viability assessed by counting in an improved Neubauer chamber using Trypan blue. Half a million  
281 viable cells were incubated with 2.5  $\mu$ l of Human TruStain FcX™ Fc Blocking Reagent (BioLegend  
282 422302), followed by 25  $\mu$ l TotalSeq-C™ antibody cocktail (BioLegend 99813).

##### 283 10X Genomics droplet single-cell RNA-sequencing

284 50,000 live cells for each pool were processed using Single Cell VDJ 5’ version 1.1 (1000020) together  
285 with Single Cell 5’ Feature Barcode library kit (1000080), Single Cell V(D)J Enrichment Kit, Human B

286 Cells (1000016) and Single Cell V(D)J Enrichment Kit, Human T Cells (1000005) from 10X Genomics  
287 following manufacturer's recommendations. The samples were subjected to 12 cycles of cDNA  
288 amplification and 8 cycles for the protein library construction. The rest of libraries were processed as  
289 indicated by the manufacturer. Libraries were pooled per sample using the ratio 9:2.4:1:0.6 for gene  
290 expression, feature barcoding, TCR enriched and BCR enriched libraries. Samples were sequenced on  
291 an Illumina NovaSeq6000 sequencer machine using S1 flowcells.

#### 292 Single-cell RNA-sequencing processing, demultiplexing and quality control

293 Multiplexed 10X scRNA-seq GEX libraries were aligned to the human genome, reads deduplicated,  
294 and UMIs quantified using Cellranger v4.0 utilising the hg38 genome reference sequence. Gene  
295 expression count matrices of genes by droplets were generated separately for each multiplex pool of  
296 donors<sup>20</sup>, demultiplexing and single cell genotypes derived using CellSNP ([https://github.com/single-](https://github.com/single-cell-genetics/cellSNP)  
297 [cell-genetics/cellSNP](https://github.com/single-cell-genetics/cellSNP)) were assigned to individual donors and quality control performed as  
298 previously described<sup>21,22</sup>. Doublets were identified using the "doubletCells" function in *scrn* based  
299 on highly variable genes (HVGs). "Cluster walktrap" (<https://arxiv.org/abs/physics/0512106>) was  
300 used on the shared nearest-neighbour (SNN)-graph that was computed on HVGs in principal  
301 component space to form highly resolved clusters per sample. Doublets were removed prior to any  
302 downstream analyses.

#### 303 Single-cell RNA-sequencing clustering and annotation

304 Highly variable genes (HVG) were defined across all single-cells and assigned to a donor individual.  
305 Single-cell clusters were computed by first constructing a k-nearest neighbour graph (k=20), and  
306 broadly grouped into discrete clusters based on the Walktrap community detection algorithm, using  
307 the kNN-graph as input. Each cluster was annotated into one of 7 broad categories based on the  
308 expression of canonical marker genes for each: CD4 T cell, CD8 Tcell, NK cell, Monocyte, Plasma cell,  
309 B cell and dendritic cell. HVGs, PCA, k-NN graph and clusters were re-computed for subsets of cells in  
310 each category, and sub clusters annotated based on marker genes.

311 Differential gene expression between clinical severity groups in Classical Monocytes, and between  
312 CD4+ Naïve and CD4+ FOXP3 Tregs in healthy controls, used the mean log normalized expression  
313 across single-cells from each individual. Mean expression values were compared in a linear model, p-  
314 values are reported from a 2-sided t-test adjusted for multiple testing using a Bonferroni correction  
315 (m=9 tests).

### 316 **RT-PCR**

317 250 ng total RNA was amplified with FV forward (5'- ACCACAATCTACCATTTTCAGGACTT -3'); FV  
318 reverse (5'- CGCCTCTGCTCACGAGTTAT -3') and Foxp3 forward (5'- GCTGCAGCTCTCAACGGT -3');  
319 Foxp3 reverse (5'- GGCAAACATGCGTGTGAAC -3') using RT-PCR system following manufacture's  
320 instruction ; the PCR product was visualized by 1% low melting temperature agarose gel in Tris-  
321 Acetate-EDTA buffer.

322

### 323 **Immunoblotting**

324 Equal number of T regs and the CD4 enriched fraction isolated from the kit described above were  
325 collected and lysates prepared for SDS polyacrylamide gel electrophoresis and immunoblotting as  
326 previously described<sup>23</sup>. Signals were detected by enhanced chemiluminescence using ECL (Thermo  
327 Scientific, Paisley, UK). Images were collected and analysed using Image Lab (Bio-Rad, Hemel  
328 Hempstead, UK).

329

### 330 **Expression of FV constructs**

331 Three constructs comprising (1) FV B domain ((aa710-1545), (2) full length FV (aa 1 - 2224) and (3)  
332 [R709A, R1018A, R1545A]FV aa1-2224 were sub-cloned into a proprietary vector for the HEK293-6E  
333 system. All sequences contained a C-terminal 6His tag to facilitate purification. Cells were  
334 transfected at a 500 ml scale for each construct, media harvested 5-6 days after transfection and  
335 protein purified using a combination of Ni affinity and size exclusion chromatography and if required

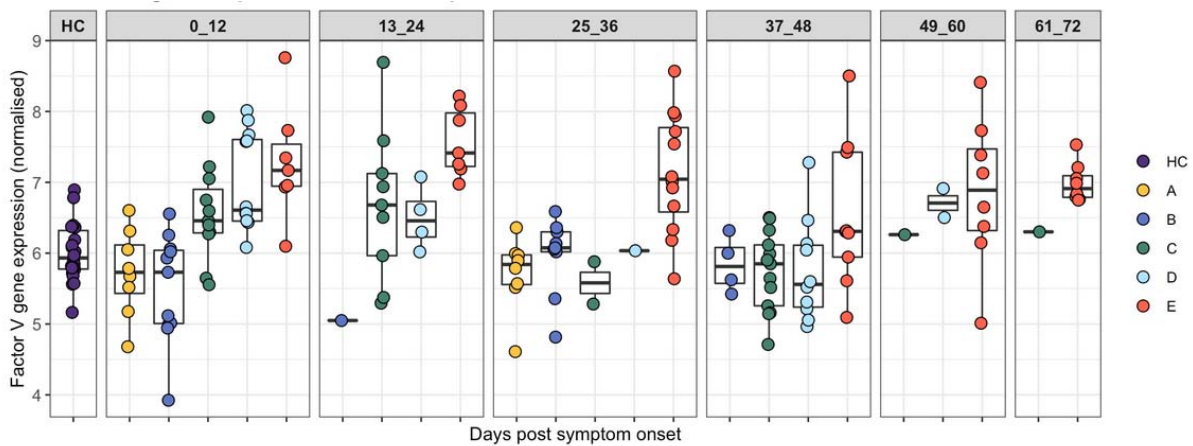
336 ion exchange. Purified proteins were analysed by reducing and non-reducing SDS-PAGE, A280 to

337 determine concentration, size exclusion and mass spectrometry to confirm identity.

338

339

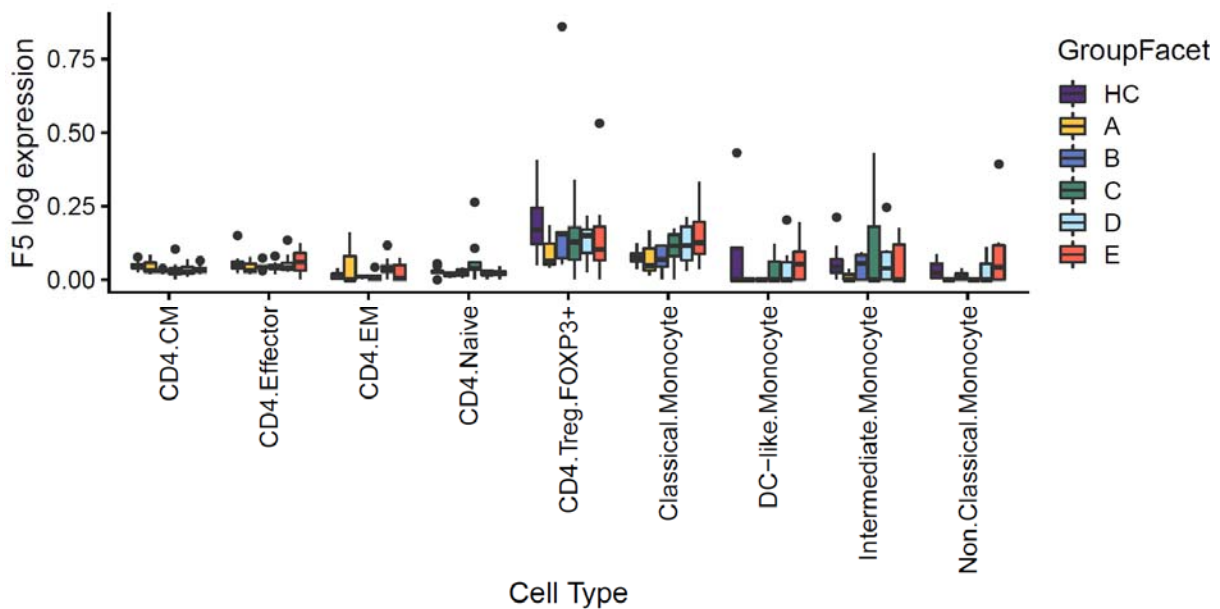
340 A.



341

342

343 B.



344

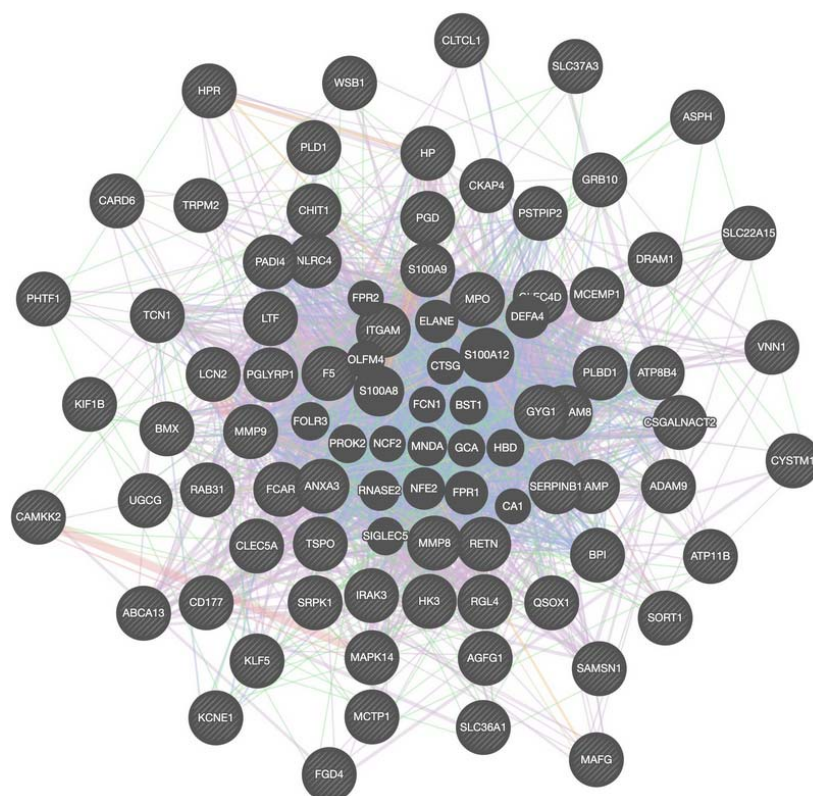
345 **Figure 1. FV is produced by circulating blood cells and increased in hospitalised patients with**  
 346 **Covid-19**

347 A. Peripheral blood cells from healthy controls, healthcare workers and patients with Covid-19  
 348 express FV. Individuals represented by dots are grouped into 12 day time periods after onset of  
 349 symptoms or a positive swab in asymptomatic healthcare workers (HCW). HC, healthy controls; A,  
 350 HCW screening asymptomatic; B, HCW screening symptomatic; C, hospitalised mild disease; D,  
 351 hospitalised requiring oxygen; E, hospitalised, intensive care. 0 to 12 days D vs HC  $p = 0.0007$ ; E vs HC  
 352  $p = 0.0002$ . 13 to 24 days E vs HC  $p = 0.00001$ . 25 – 36 days E vs HC  $p = 0.00003$ . 49 to 60 days E vs  
 353 HC  $p = 0.013$ . 61 to 72 days E vs HC  $p = 0.00003$ .

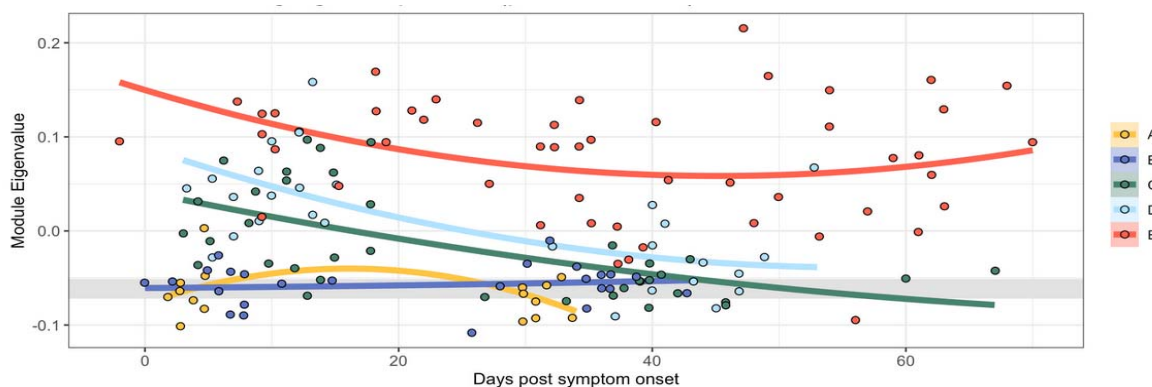
354 B. scRNAseq of PBMCs derived from HC, HCW and patients with Covid-19 showed the highest  
 355 expression of FV in CD4+, FoxP3+ Tregs, with expression also detected in monocytes and at lower  
 356 levels in other CD4 cell subsets. FV expression was increased in CD4+ Naive vs CD4+ FOXP3 Tregs in  
 357 healthy controls ( $p = 8.33 \times 10^{-4}$ ), and in severe Covid-19 vs healthy controls in classical monocytes but  
 358 not other cell subsets ( $p = 0.016$ ).



359 A.



360 B.

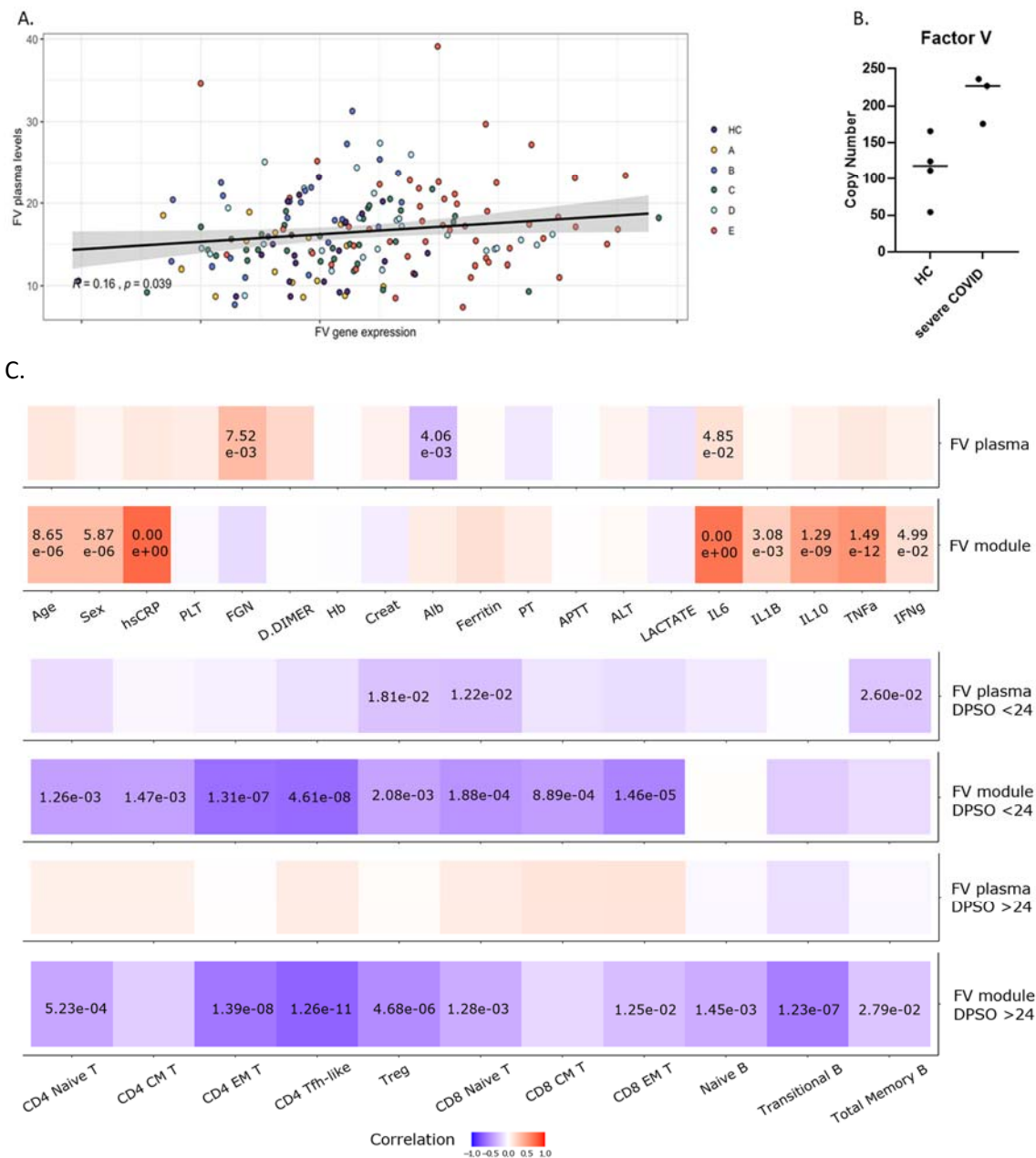


361  
362

363 **Figure 2. In peripheral blood cells FV is co-expressed with a module of genes expressed in**  
364 **neutrophils, and expression of the module correlates with severity of Covid-19**

365 A. Weighted gene co-expression network analysis identified a module containing group of genes co-  
366 expressed with FV. In this module FV is a hub gene and its expression correlates strongly with genes  
367 expressed in neutrophils. The lines are colour coded to show relationships. Purple: Gene known to  
368 be co-expressed in existing gene databases. Orange: Predicted functional relationships between  
369 genes. Pink: Proteins known to be linked. Turquoise: Genes present in a shared annotated pathway.  
370 Blue: Genes expressed in the same tissue. B. Mixed-effects model with quadratic time trend showing  
371 the longitudinal expression of the FV module over time, grouped by severity. Grey band indicates  
372 the interquartile range of HCs. A significant effect of time versus severity group interaction term ( $p =$   
373  $0.0047$ ) indicates that disease severity has a significant effect on longitudinal expression. A, HCW  
374 screening asymptomatic; B, HCW screening symptomatic; C, hospitalised mild disease; D,  
375 hospitalised requiring oxygen; E, hospitalised, intensive care.

376  
377



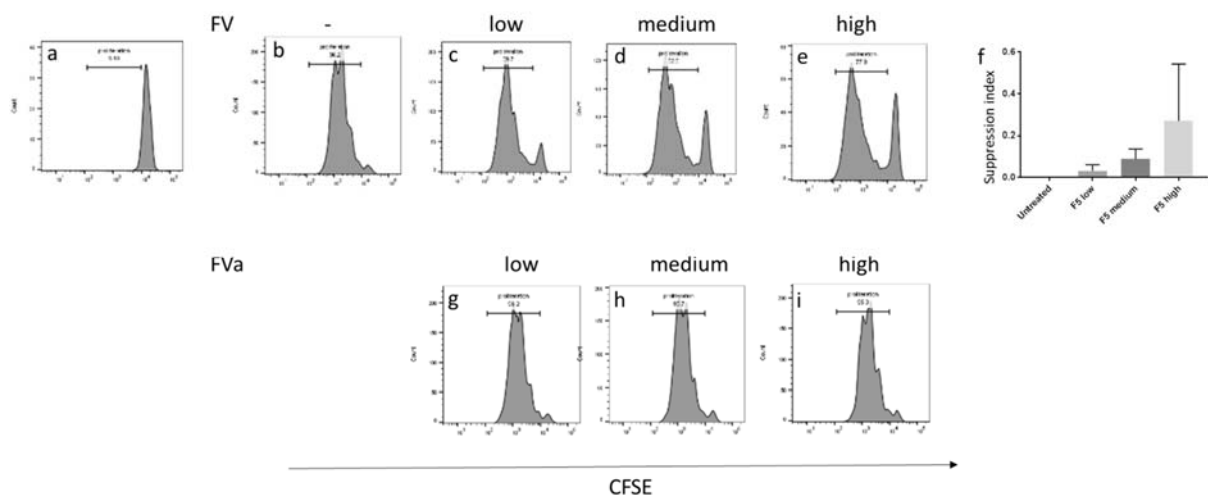
378  
379  
380  
381  
382  
383  
384  
385  
386  
387  
388  
389  
390  
391  
392  
393

**Figure 3. FV expression correlates with parameters of disease severity and lymphopenia**

A. Correlation of plasma FV levels and peripheral blood cell FV gene expression in healthy controls and patients with Covid-19 ( $r=0.16$ ,  $p = 0.039$ ).

B. LC-MS measurement of FV in protein lysates of neutrophil extracts from healthy controls and patients with severe Covid-19. FV levels were significantly higher in neutrophil lysates from patients with severe Covid-19 compared to healthy ( $p = 0.025$ ).

C. Correlation of plasma FV levels and FV module gene expression with predictors of disease severity and plasma protein levels (i-ii); or with B and T cell counts (iii-vi). FV plasma levels correlate with fibrinogen and IL6 (i), whereas FV module gene expression correlated with predictors of disease severity (age, male gender, CRP) and increased plasma levels of IL6, IL10 and TNF (ii). There was very little correlation between plasma factor V levels and T and B cell counts during the first 24 days post symptom onset (DPSO, iii) or after 24 days from the onset of symptoms (v). In contrast, FV module gene expression correlates with suppression of T cell counts during the first 24 days post symptom onset (iv), and T and B cell counts after 24 days from the onset of symptoms (vi). p values are shown where significant.



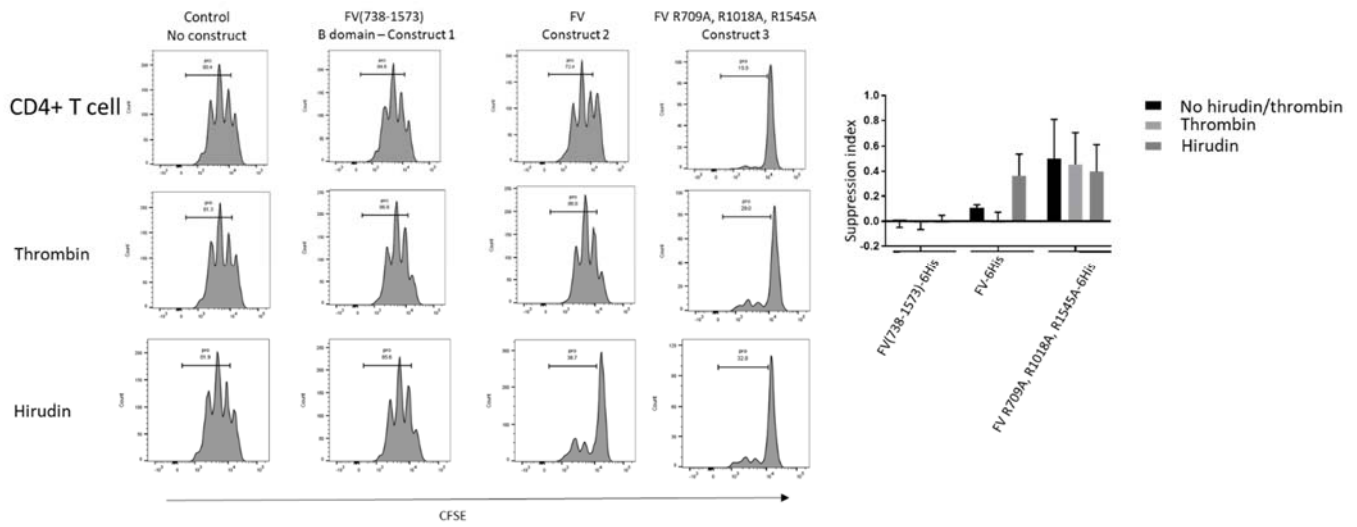
394  
395

396 **Figure 4. FV suppresses T cell proliferation**

397 CD4+T conventional cells (Tcon) were labelled with carboxyfluorescein diacetate succinimidyl ester  
398 (CFSE) (a), and stimulated with Dynabeads T cell activator, proliferation was shown as diluting the  
399 dye and reducing fluorescence intensity (b). Proliferation is inhibited in a concentration dependent  
400 manner by addition of native Factor V (panels c – e), but not by activated factor V, FVa (g – i). Data  
401 are representative of 10 healthy donors (f), FV at medium concentration suppressed T cell  
402 proliferation by 3 to 17 percent ( $p=0.0003$ ). Medium concentration is close to the physiological  
403 plasma level at 20 nM, low concentration is 4 nM, high concentration is 100 nM.  
404

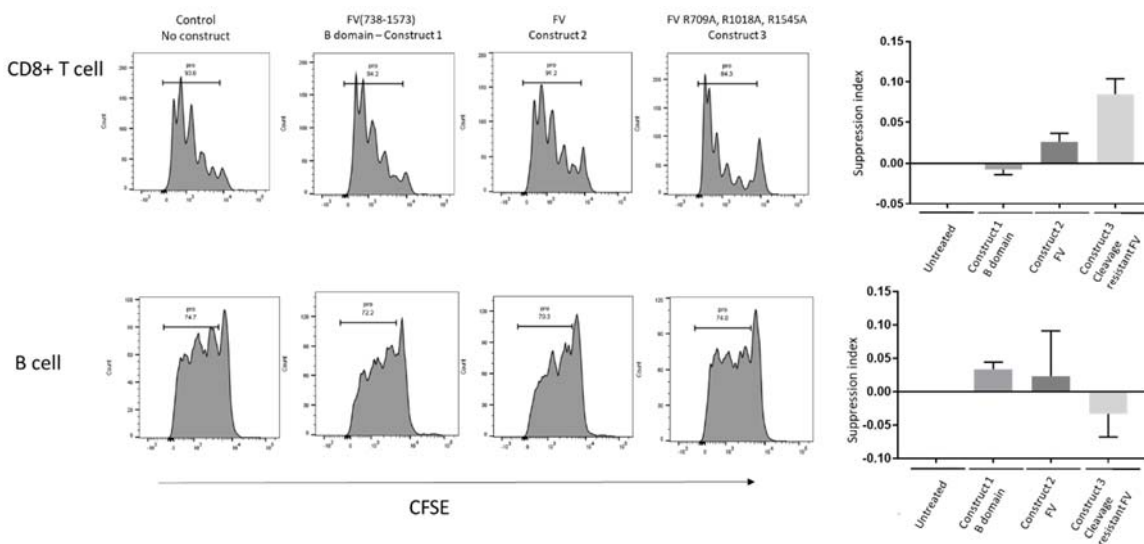
405  
406

A.



407  
408

409 B.



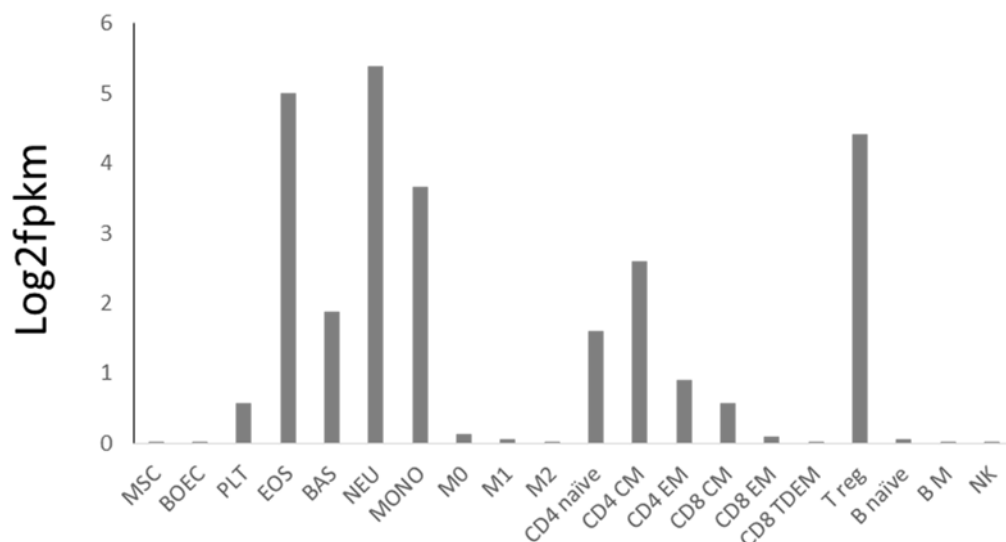
410  
411

**Figure 5. Full length, but not thrombin cleaved FV, suppresses T but not B cell proliferation**

413 A. Tcon proliferation was not inhibited by recombinant FV B domain (Construct 1), and thrombin and  
414 hirudin had no effect on their own and in combination with construct 1. Recombinant full length  
415 Factor V (construct 2) inhibited Tcon proliferation similar to native plasma derived Factor V,  
416 and its effect was prevented by thrombin ( $p=0.036$ ), while the effect of inhibition by mutated Factor V  
417 (construct 3) was not prevented by thrombin ( $p=0.25$ ).

418 B. CD8+ T cell proliferation was inhibited similarly by construct 2 ( $p=0.009$ ) and construct 3  
419 ( $p=0.004$ ), while B cell proliferation was not inhibited by any of the constructs ( $p=0.1$ ;  $p=0.3$ ;  $p=0.6$ ).  
420 Pro: proliferation.

421

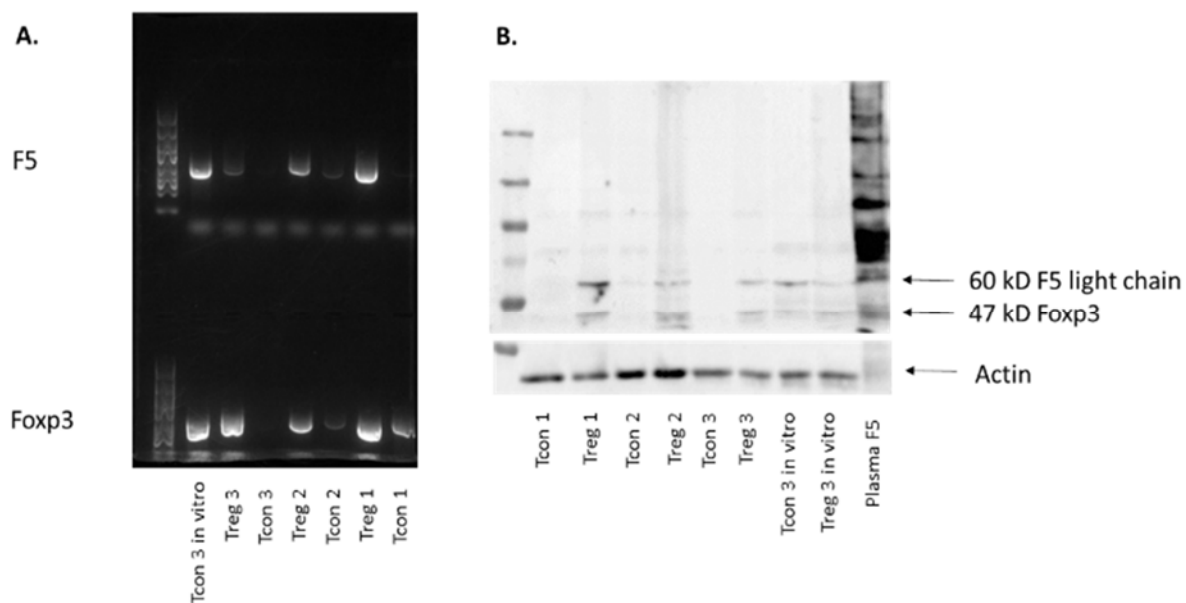


422  
423  
424  
425  
426  
427  
428  
429  
430  
431  
432  
433

Supplementary Figure 1.

Analysis of the Blueprint (<https://www.blueprint-epigenome.eu/>) database identified FV expression in peripheral blood cell subsets in healthy individuals, with the highest expression in neutrophils, eosinophils, monocytes and Tregs derived from healthy individuals. fpkm - fragments per kilobase of transcript per million mapped reads. MSC: mesenchymal stem cells, BOEC: blood outgrowth endothelial cells, PLT: platelet, EOS: eosinophil, BAS: basophil, NEU: neutrophil, MONO: monocyte, M0, M1 and M2: macrophages, CM: central memory, EM: effector memory, TDEM: terminally differentiated effector memory, T reg: regulatory T cells, B M: B memory NK: natural killer.

434  
435

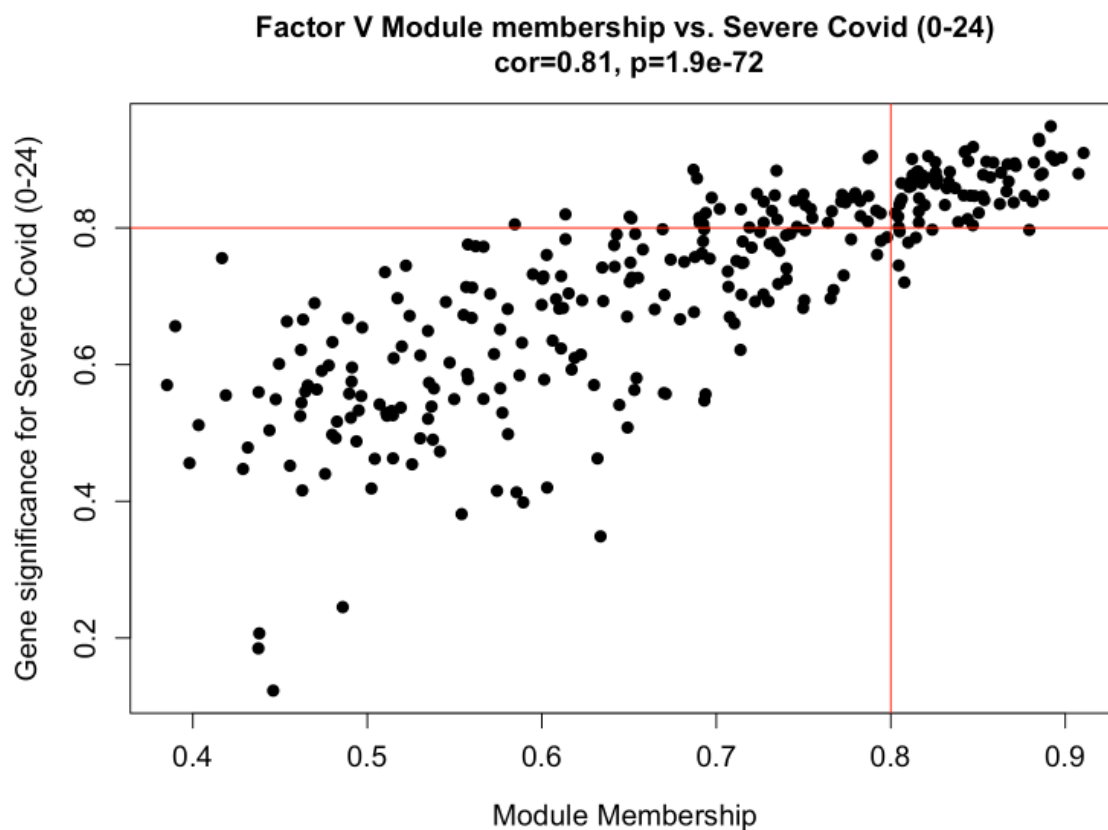


436  
437  
438  
439  
440  
441  
442

Supplementary Figure 2.

Expression of FV in Tregs, and also *in vitro* expanded T cells, was confirmed by Rt-PCR (A), and immunoblotting (B).

443  
444



445  
446  
447

448 Supplementary Figure 3.

449 Factor V module membership vs gene significance for severe Covid-19.

450 Genes comprising the Factor V module are graphed. The x axis represents the correlation of a given  
451 gene's expression with the module eigenvalue. The higher the correlation, the more representative  
452 the module expression is of the gene. The Y axis represents the correlation between a gene's  
453 expression and disease status (HC versus severe Covid-19 at 0-12 days post symptom onset). The  
454 higher the correlation, the more able a given gene can distinguish severe Covid-19 from health. The  
455 red lines demarcate the "hub genes" which represent genes that strongly model the module and  
456 disease status. The genes illustrated in Figure 2A are: KIF1B; PGD; PADI4; SORT1; PHTF1; SLC22A15;  
457 S100A9; F5; QSOX1; CHIT1; MTARC1; NLRC4; AGFG1; LTF; CAMP; GYG1; PLD1; ATP11B; ANXA3;  
458 CARD6; MCTP1; CYSTM1; SLC36A1; HK3; SERPINB1; SRPK1; MAPK14; VNN1; ABCA13; GRB10;  
459 SLC37A3; CLEC5A; BMX; ADAM9; ASPH; UGCG; LCN2; TCN1; MMP8; CSGALNACT2; CLEC4D; PLBD1;  
460 FGD4; IRAK3; DRAM1; CKAP4; CAMKK2; KLFV; ATP8B4; ITGAM; HP; HPR; WSB1; MPO; MAFG; RAB31;  
461 PSTPIP2; BPI; MMP9; RETN; MCEMP1; CEACAM8; CD177; PGLYRP1; FCAR; CLTCL1; RGL4; TSPO;  
462 SAMS1; KCNE1; TRPM2.

463  
464

465  
466

- 467 1. Zhou, T., Su, T.T., Mudianto, T. & Wang, J. Immune asynchrony in COVID-19 pathogenesis  
468 and potential immunotherapies. *J Exp Med* **217**(2020).
- 469 2. Bikdeli, B., *et al.* COVID-19 and Thrombotic or Thromboembolic Disease: Implications for  
470 Prevention, Antithrombotic Therapy, and Follow-Up: JACC State-of-the-Art Review. *J Am Coll*  
471 *Cardiol* **75**, 2950-2973 (2020).
- 472 3. Stefely, J.A., *et al.* Marked factor V activity elevation in severe COVID-19 is associated with  
473 venous thromboembolism. *Am J Hematol* **95**, 1522-1530 (2020).
- 474 4. Shen, N.L., *et al.* The serine protease cofactor factor V is synthesized by lymphocytes. *J*  
475 *Immunol* **150**, 2992-3001 (1993).
- 476 5. Dashty, M., *et al.* Characterization of coagulation factor synthesis in nine human primary cell  
477 types. *Sci Rep* **2**, 787 (2012).
- 478 6. Spyropoulos, A.C. & Weitz, J.I. Hospitalized COVID-19 Patients and Venous  
479 Thromboembolism: A Perfect Storm. *Circulation* **142**, 129-132 (2020).
- 480 7. Bikdeli, B., *et al.* COVID-19 and Thrombotic or Thromboembolic Disease: Implications for  
481 Prevention, Antithrombotic Therapy, and Follow-Up: JACC State-of-the-Art Review. *J Am Coll*  
482 *Cardiol* **75**, 2950-2973 (2020).
- 483 8. Shen, B., *et al.* Proteomic and Metabolomic Characterization of COVID-19 Patient Sera. *Cell*  
484 **182**, 59-72.e15 (2020).
- 485 9. Ronit, A., *et al.* Compartmental immunophenotyping in COVID-19 ARDS: A case series. *J*  
486 *Allergy Clin Immunol* (2020).
- 487 10. Radermecker, C., *et al.* Neutrophil extracellular traps infiltrate the lung airway, interstitial,  
488 and vascular compartments in severe COVID-19. *J Exp Med* **217**(2020).
- 489 11. Veras, F.P., *et al.* SARS-CoV-2-triggered neutrophil extracellular traps mediate COVID-19  
490 pathology. *J Exp Med* **217**(2020).
- 491 12. Zheng, M. & Tian, Z. Liver-Mediated Adaptive Immune Tolerance. *Front Immunol* **10**, 2525  
492 (2019).



- 493 13. Hasan, S.S., Radford, S., Kow, C.S. & Zaidi, S.T.R. Venous thromboembolism in critically ill  
494 COVID-19 patients receiving prophylactic or therapeutic anticoagulation: a systematic review  
495 and meta-analysis. *J Thromb Thrombolysis* **50**, 814-821 (2020).
- 496 14. Olson, S.T., Richard, B., Izaguirre, G., Schedin-Weiss, S. & Gettins, P.G. Molecular  
497 mechanisms of antithrombin-heparin regulation of blood clotting proteinases. A paradigm  
498 for understanding proteinase regulation by serpin family protein proteinase inhibitors.  
499 *Biochimie* **92**, 1587-1596 (2010).
- 500 15. Nutescu, E.A., Burnett, A., Fanikos, J., Spinler, S. & Wittkowsky, A. Pharmacology of  
501 anticoagulants used in the treatment of venous thromboembolism. *J Thromb Thrombolysis*  
502 **41**, 15-31 (2016).
- 503 16. Wallin, R. & Hutson, S.M. Warfarin and the vitamin K-dependent gamma-carboxylation  
504 system. *Trends Mol Med* **10**, 299-302 (2004).
- 505 17. Gorski, A., Wasik, M., Nowaczyk, M. & Korczak-Kowalska, G. Immunomodulating activity of  
506 heparin. *FASEB J* **5**, 2287-2291 (1991).
- 507 18. Collier, D.A., *et al.* Point of Care Nucleic Acid Testing for SARS-CoV-2 in Hospitalized Patients:  
508 A Clinical Validation Trial and Implementation Study. *Cell Rep Med* **1**, 100062 (2020).
- 509 19. Kim, D., Paggi, J.M., Park, C., Bennett, C. & Salzberg, S.L. Graph-based genome alignment and  
510 genotyping with HISAT2 and HISAT-genotype. *Nat Biotechnol* **37**, 907-915 (2019).
- 511 20. Lun, A.T.L., *et al.* EmptyDrops: distinguishing cells from empty droplets in droplet-based  
512 single-cell RNA sequencing data. *Genome Biol* **20**, 63 (2019).
- 513 21. Huang, Y., McCarthy, D.J. & Stegle, O. Vireo: Bayesian demultiplexing of pooled single-cell  
514 RNA-seq data without genotype reference. *Genome Biol* **20**, 273 (2019).
- 515 22. Lun, A.T., McCarthy, D.J. & Marioni, J.C. A step-by-step workflow for low-level analysis of  
516 single-cell RNA-seq data with Bioconductor. *F1000Res* **5**, 2122 (2016).
- 517 23. Wang, J., *et al.* TNFR2 ligation in human T regulatory cells enhances IL2-induced cell  
518 proliferation through the non-canonical NF-kappaB pathway. *Sci Rep* **8**, 12079 (2018).

519 **Acknowledgements**

520 This work was supported by the NIHR BioResource, the NIHR Cambridge Biomedical Research Centre  
521 and the NIHR Cambridge Clinical Research Facility. FV plasma assays were performed by the NIHR  
522 Cambridge Biochemical Assay Laboratory. FV constructs were prepared and expressed by Peak  
523 Proteins. Neutrophil proteins were characterised at the Mass Spectrometry Facility at the University  
524 of Dundee and the QMRI flow cytometry and cell sorting facility. Sequencing was supported by Paul  
525 Coupland from the CRUK Cambridge Institute Genomics Core.

526 The work was funded by awards from NIHR to the NIHR BioResource and the NIHR Cambridge  
527 Biomedical Research Centre, Evelyn Trust, UKRI/NIHR funding through the UK Coronavirus  
528 Immunology Consortium (UK-CIC) and a CSO award (COV/DUN/20/01). KGCS holds a Wellcome Trust  
529 Investigator award. BG holds an award from the Aging Biology Foundation Europe to BG. RKG holds a  
530 Wellcome Senior Fellowship (WT108082AIA). PK is supported by the Australian and New Zealand  
531 Society of Nephrology and the Royal Australasian College of Physicians. SRW holds a Wellcome Trust  
532 Senior Clinical Fellowship (209220). ERW holds a Wellcome Clinical Training Fellowship award  
533 (108717/Z/15/Z). NM was supported by a DFG Research Fellowship. PFC is a Wellcome Trust  
534 Principal Research Fellow (212219/Z/18/Z), and a NIHR Senior Investigator, and receives support  
535 from the Medical Research Council (MRC) Mitochondrial Biology Unit, the MRC International Centre  
536 for Genomic Medicine in Neuromuscular Disease, the Leverhulme Trust, a MRC research grant, and  
537 an Alzheimer's Society Project Grant. JAN holds a Wellcome Trust Senior Research Fellowship  
538 (215477/Z/19/Z).

539

540 **Declaration of interests**

541 RKG acts as a consultant for UMOVIS lab. A priority patent covering part of this work has been filed.

542

543

544

545 **Authors contributions**

546 Conceptualisation JB, JSP, JW, PAL, KGCS data collection JW, PK, PAL, FM, LB, LT, KS, NW data  
547 curation JW, PK, FM, LB, LT, NW, KS, BG, JCM formal analysis JW, PK, MDM, NW, BG, JCM funding  
548 acquisition JB, PFC, NK, PAL, KGCS investigation JW, PK, PAL, FM, LB, LT, MDM, FJC-N, KB, NM, NKW,  
549 ERW, RKG, MT, MPW, JAN, SRW, KGCS methodology and study design JW, PK, PAL, MDM, FJC-N, KB,  
550 NM, NKW, ERW, PFC, NK, SP,KS, NW, RKG, MT, MPW, SRW, WHO, BG, MK, KGCS, JSP, JRB writing –  
551 original draft JW, PK, JSP, MDM writing – review & editing JW, PK, PAL, FM, LB, LT, RSA-L, MDM, FJC-  
552 N, KB, NM, NKW, ERW, PFC, NK, SP,KS, NW, RKG, MT, MPW, SRW, WHO, BG, MK, KGCS, JSP, JRB  
553